WAVE PROPAGATION IN MULTILAYER STRUCTURES AND ADVANCED STRUCTURAL THEORIES

Serge Abrate[1] and Roberta Massabò[2]

[1]Mechanical Engineering and Energy Processes
Southern Illinois University, Carbondale, IL 62901-6603, USA
Email: abrate@engr.siu.edu

[2]Department of Civil, Chemical and Environmental Engineering,
University of Genova, Genova, 16145, Italy
Email: roberta.massabo@unige.it

Keywords: Composite plates, Modal analysis, Identification, Properties, Finite elements

ABSTRACT

The dynamic behaviour of laminated structures with imperfect interfaces is studied by considering the propagation of harmonic waves. Interfaces are assumed to allow for relative motion in both the tangential and normal directions. New models are developed for studying basic cases and the fundamentals of the problem, a new and efficient zigzag theory is used to analyse laminates with an arbitrary number of layers. This work is applicable to laminated composite structures, sandwich structures, laminated glass and other laminated structures. The work points out the challenges associated with modelling laminates with imperfect bonding and the limitations of several existing theories, particularly for dynamic problems.

1 INTRODUCTION

This study is focused on layered beams with imperfect interfaces so that relative motion occurs in both the tangential and the normal directions. To determine the influence of these imperfections on the behavior of the beam we examine the propagation of harmonic waves. This work is applicable to laminated composite structures which often have a resin rich zone between layers, sandwich structures, laminated glass, and also nano-composites. It is also applicable to these structures in the presence of interfacial damage and delaminations.

Studies in this area started with the work on Newmark et al [1] who considered steel–concrete composite beams with an elastic shear connection between the two elastic materials and showed the importance of the relative slip between the two portions of the beam. Several individual pieces of lumber can be joined together using adhesives or nails to form a laminated beam. Typically all the layers are assumed to have the same transverse displacement but are assumed to slip at the interface. Bohnhoff [2] represents each layer by a conventional frame finite element. Nail elements connecting the layers above and below the interfaces are linear springs connecting the neutral axes of those layers in the axial direction. With laminated glass, stiff glass layers are connected by a soft polymeric layer and the same kinematic assumption is made: the glass layers have the same transverse displacement and curvature and the interlayer provides coupling of the axial displacements of the layers above and below. Some studies consider geometrical nonlinearities by including von Karman type terms in the strain-displacement relations (e.g. [3]) or the viscoelastic behaviour of the interlayer (e.g. [4]). Generally the transparent elastomeric interlayer is elastic for short duration (less than 60 s) loading and viscoelastic under long-duration loading [5][6]. Imperfectly bonded interfaces in laminated composite structures have been considered since the late 1990s (e.g. [7][8]). Zig-zag approaches have been proposed, and later perfected [9] to treat problems with a large number of layers and imperfect interfaces using the same number of variables of classical single-layer theories. Adekola [10] was the first to consider the relative motion in the direction normal to the interface so that layers above and below the interface no longer have the same curvature.

Section 2 develops a simple but general approach for elastically connected double beams with relative motion in the tangential and normal at the interface. Application to sandwich structures are discussed in Section 3 and Section 4 discusses wave propagation in multilayer structures with imperfect interfaces modelled using a new and improved zigzag theory.

2 TWO LAYER BEAM WITH ELASTIC INTERFACE

Consider two elastic beams separated by an elastic interface. In the following, properties of the top and bottom beams are denoted by the subscripts 1 and 2 respectively. Fig. 1 shows a free body diagram of a small segment of length Δx for the top beam. N_1 is the axial force, V_1 is the shear force, M_1 is the bending moment, and T_T and T_N are forces per unit length in the tangential and normal directions.

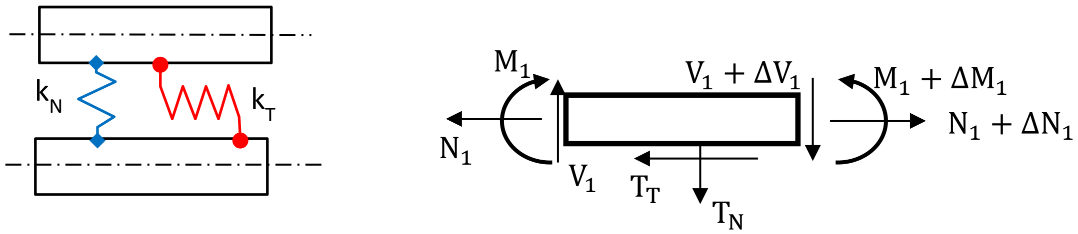

Figure 1: Free body diagram of a small element of the top beam in a two-layer beam

The equations of motion of this beam are

$$N_{1,x} - T_T = \rho_1 A_1 \ddot{u}_1^o \qquad -V_{1,x} - T_N = \rho_1 A_1 \ddot{w}_1 \qquad M_{1,x} - V_1 - \frac{h_1}{2} T_T = \rho_1 I_1 \ddot{\psi}_1 \quad (1\text{-}3)$$

where u_1^o is the longitudinal displacement of the neutral axis, w_1 is the transverse displacement , and ψ_1 is the rotation of the cross section. Using the kinematics of the Timoshenko beam theory, the axial displacement at an arbitrary point is given by $u_1 = u_1^o - z\psi_1$, and the beam constitutive equations are

$$N_1 = E_1 A_1 u_{1,x}^o \qquad M_1 = E_1 I_1 \psi_{1,x} \qquad V_1 = G_1 A_1 \left(\psi_1 - w_{1,x}\right) \quad (4\text{-}6)$$

The relative displacements at the interface between the two beams are $\delta_N = w_1^o - w_2^o$ in the normal direction and $\delta_T = u_1^o - u_2^o + \frac{h_1}{2}\psi_1 + \frac{h_2}{2}\psi_2$ in the transverse direction. The interface forces are $T_N = k_N \delta_N$ and $T_T = k_T \delta_T$. For the lower beam (beam 2) the equations of motion are

$$N_{2,x} + T_T = \rho_2 A_2 \ddot{u}_2^o \qquad -V_{2,x} + T_N = \rho_2 A_2 \ddot{w}_2 \qquad M_{2,x} - V_2 - \frac{h_2}{2} T_T = \rho_2 I_2 \ddot{\psi}_2 \quad (7\text{-}9)$$

The constitutive equations for beam 2 are obtained by changing subscripts 1 to 2 in Eqs. 4-6. These equations describe the behavior of two Timoshenko beams coupled by an elastic interface allowing motion in both the tangential and normal direction. In the remainder of this section, the dynamic behavior of beams on elastic foundation, Timoshenko beams, and elastically connected beams is examined.

2.1 Bernoulli-Euler beam on elastic foundation

For a Bernoulli-Euler beam $\psi_1 = w_{1,x}$, $\rho_1 I_1 = 0$ and, beam 2 being rigid, the motion is governed by

$$E_1A_1\, u^o_{1,xx} - k_T\left(u^o_1 + \frac{h_1}{2} w_{1,x}\right) = \rho_1 A_1\, \ddot{u}^o_1 \tag{10}$$

$$E_1I_1\, w_{1,xxxx} + \rho_1 A_1 \ddot{w}_1 + k_N w_1 - \frac{h_1}{2} k_T\left(u^o_{1,x} + \frac{h_1}{2} w_{1,xx}\right) = 0 \tag{11}$$

Consider three cases:

1. Case 1: k_T=0, Eq. 10 becomes the wave equation $(E_1A_1\, u^o_{1,xx} = \rho_1 A_1\, \ddot{u}^o_1)$ and Eq. 11 becomes the equation of motion for a beam on a Winkler foundation $(E_1I_1\, w_{1,xxxx} + \rho_1 A_1 \ddot{w}_1 + k_N w_1 = 0)$.
2. Case 2: $k_T \neq 0$ but the top and bottom beams are assumed to be connected at their neutral axes (Fig. 2.a) as in [2]. The tangential slip is $\delta_T = u^o_1 - u^o_2$ with $u^o_2 = 0$ for the present case and the 4^{th} term in Eq. 11 disappears since T_T no longer creates a bending moment. Eq. 10 becomes $E_1A_1\, u^o_{1,xx} - k_T\, u^o_1 = \rho_1 A_1\, \ddot{u}^o_1$ and Eq. 11 is that of a BE beam on a Winkler foundation. The axial and transverse motions are still uncoupled.
3. Case 3: fully coupled case (Fig. 1.a) governed by Eqs. (10, 11)

For harmonic waves with frequency ω and wave number k propagating in this rod, $u^o_1 = U_1 \exp\{i(kx - \omega t)\}$ and $w_1 = W_1 \exp\{i(kx - \omega t)\}$. The wave number is related to the wavelength λ by $k = 2\pi/\lambda$ and the phase velocity c= ω /k. The radius of gyration of the cross section ($r = \sqrt{I/A}$) is used in the presentation of the results (Fig. 2). For a beam on elastic foundation, the presence of the foundation affects the bending behavior for long wavelengths (Fig. 2.b) and for the fully coupled case both coupling constants affect the behavior even if the results (Fig. 2.c) appear qualitatively similar. In Fig. 2.c, the line labelled NF is for the case of a beam with no foundation (k_N=k_T=0).

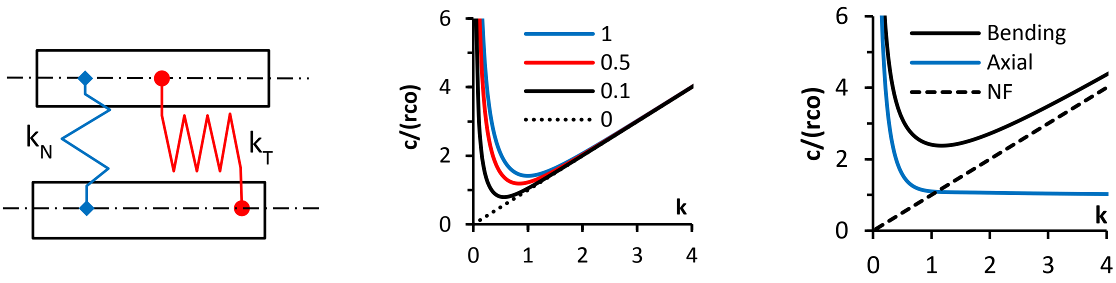

(a) (b) (c)

Figure 2: (a) normal and shear coupling for Case 2; (b) effect of foundation modulus on phase velocity for beam on Winkler foundation (k_N/EA=0, 0.1, 0.5, 1; r=1); (c) fully coupled model (k_N/EA=k_T/EA=1; r=1)

This example shows the effect of assumptions on the coupling between the two beams (Figs. 1.a, 2.a) and the effect of the two elastic constants k_T and k_S. Results show that the effect of the foundation is important for long wavelengths.

2.2 Elastically connected rods

With the elastic coupling model used in subsection 2.1 (Fig. 2.a) where $\delta_T = u_1^o - u_2^o$, axial and bending motions are uncoupled. The equations of motion for two coupled rods are

$$E_1A_1\, u_{1,xx}^o - k_T\left(u_1^o - u_2^o\right) = \rho_1 A_1 \ddot{u}_1^o, \qquad E_2A_2\, u_{2,xx}^o + k_T\left(u_1^o - u_2^o\right) = \rho_2 A_2 \ddot{u}_2^o \tag{12}$$

for axial motion and for bending,

$$E_1I_1\, w_{1,xxxx} + \rho_1 A_1 \ddot{w}_1 + k_N\left(w_1 - w_2\right) = 0, \qquad E_2I_2\, w_{2,xxxx} + \rho_2 A_2 \ddot{w}_2 - k_N\left(w_1 - w_2\right) = 0 \tag{13}$$

There is an extensive literature on elastically coupled beams governed by these equations. To cite only two references: [11] deals with the longitudinal motion of elastically connected bars and multiple beams governed by Eqs. 13 are considered in [12]. Usually all the beams are assumed to be identical. For harmonic waves with frequency ω and wave number k propagating in a coupled rod system, $u_1^o = U_1 \exp\left\{i\left(kx - \omega t\right)\right\}$ and $u_2^o = U_2 \exp\left\{i\left(kx - \omega t\right)\right\}$. Substituting into Eqs. 12 gives the dispersion relation

$$\left(E_1A_1\, k^2 + k_T - \rho_1 A_1 \omega^2\right)\left(E_2A_2\, k^2 + k_T - \rho_2 A_2 \omega^2\right) - k_T^2 = 0 \tag{14}$$

When the two bars are identical, there are two wave propagation modes: (a) the first one with frequency $\omega = c_o k$ where $c_o = \sqrt{E/\rho}$ and $U_1 = U_2$ so the two bars move in phase; (b) for the second mode $\omega^2 = c_o^2 k^2 + \left(2k_T/\rho A\right)$, $U_1 = -U_2$, and the bars move in opposite phase. For long waves the cut-off frequency given by $\omega_{co}^2 = 2k_T/\rho A$ shows the effect of the elastic coupling. For short waves both modes have essentially the same phase velocity c_o which is often called the bar velocity.

Similarly, for two elastically coupled identical beams, substituting $w_1 = W_1 \exp\left\{i\left(kx - \omega t\right)\right\}$ and $w_2 = W_{21} \exp\left\{i\left(kx - \omega t\right)\right\}$ into Eqs. 13 gives two types of harmonic waves: (a) for the first mode $\omega^2 = EI\, k^4/\rho A$ and $W_1 = W_2$; (b) for the second mode, $\omega^2 = \left(EI\, k^4 + 2k_N\right)/\rho A$ and $W_1 = -W_2$. As in the case of axial motion, the two beams move in phase for the first mode and in opposite phase for the second mode.

2.3. Wave propagation in Timoshenko beams

Here we study the propagation of harmonic waves in a single isotropic beam modeled using Timoshenko's first order shear deformation theory. When $T_N = T_T = 0$, using Eqs. 5,6, the equations of motion (Eqs. 2,3) are those from the Timoshenko beam theory. The dispersion relations for Timoshenko beam theories can be written as

$$\rho A \rho I \omega^4 - \omega^2\left\{\rho A\left(GA + EIk^2\right) + \rho I GA k^2\right\} + GA\, EI k^4 = 0 \tag{15}$$

For a homogeneous beam, after some algebraic manipulations, in terms of the phase velocity c,

$$r^2k^2\, c^4 - c^2\left\{\left(c_s^2 + c_o^2 r^2 k^2\right) + c_s^2 r^2 k^2\right\} + c_s^2\, c_o^2 r^2\, k^2 = 0 \tag{16}$$

where $r = \sqrt{I/A}$ is the radius of gyration of the cross-section, $c_o = \sqrt{E/\rho}$ is the bar velocity, $c_s = \sqrt{G/\rho}$ is the shear wave velocity. Therefore, rk is a non-dimensional parameter and Eq. 16. can be used to plot c/c_o as a function of rk (Fig. 3). $c_o^2 = 2(1+\nu)c_s^2$ and a Poisson's ratio of 0.3 was used. The blue line in Fig. 3 is the dispersion relation $c = c_o rk$ for BE beams. The dispersion curves for the Timoshenko beam (in red) consist of two branches: (1) the lower branch or acoustic branch is initially tangent to the dispersion curve of the BE beam and tends to the shear wave velocity c_s for short waves; (2) the upper branch or optical branch tends to the bar velocity c_o for short waves and for long waves c becomes infinite which correspond to a cut-off frequency $\omega_{co} = \sqrt{GA/\rho I} = c_s / r$ from Eq. 15. For Timoshenko beams, the first mode is known to be a good approximation to the first anti-symmetric Lamb mode (A_o mode) for waves propagating in an elastic layer. However, for short waves the phase velocity of the A_o-mode tends to that of Rayleigh waves which is slightly lower than cs. This is why a shear correction factor κ is usually used for the shear rigidity $(GA \to GA\,\kappa)$. The second mode does not approximate the next anti-symmetric mode (A_1-mode) which is obvious since it tends to c_o whereas anti-symmetric modes tend to c_s. Studies of the vibration of TBs concluded that "predictions above the cut-off frequency should be disregarded" [13]. A discussion of the treatment of the second mode of the TB can be found in [14].

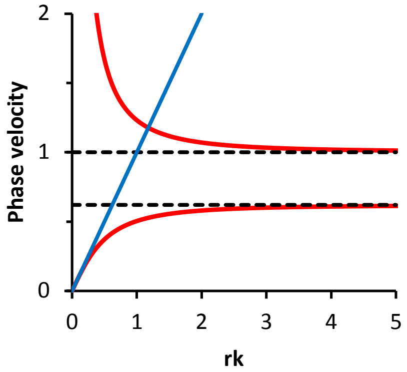

Figure 3: Non-dimensional phase velocity c/c_o versus rk, the product of the radius of gyration r and the wave number k for a homogeneous Timoshenko beam. Blue line: BE beam theory, Red lines: TB beam theory.

The phase velocity predicted by the BE beam theory is less than 5% higher that than predicted by the TB theory when $rk<0.17$ or $\lambda>37r$. For a rectangular cross section this means that the wavelength should be more than 10.68 times the height of the beam, a result to keep in mind in developing models for sandwich structures or laminates with imperfect interfaces.

3 SANDWICH STRUCTURES

Sandwich structures can be seen as two layers of noble material held together by a much lighter and more flexible core. Many theories assumed that the kinematics of the deformation of the facings can be represented by those of the Bernoulli-Euler beam theory or the Timoshenko beam theory. Similarly, for plates the assumptions of the Kirchhoff-Love or the Mindlin plate theories are used model the facings. Many levels of approximation are used to describe the deformation of the core. In the following we first examine the dynamic behaviour of sandwich beams with shear flexible cores that do not deform in the transverse direction. Then we discuss how the approach described in section 2 can be used to analyse cases with cores that are also soft in the transverse direction.

3.1 Sandwich beams with antiplane core

Sandwich structures have been studied extensively for many years since the concept originated in 1849 and the first research paper was published by Marguerre in 1944 [15]. Here we compare several sandwich beam theories on the basis of dispersion curves for harmonic wave propagation. Mead [16] re-derived and compared several theories including the simplified Yan Dowell (SYD) theory, and the

Di Taranto, Mead, Markus (DTMM) theory. The SYD and DTMM theories assume that the facings deform like BE beams and that the core is rigid in the transverse direction. The kinematics of the deformation is given by $u_1 = u_1^o - z w_{,x}$ for the top facesheet, $u_3 = u_3^o - z w_{,xx}$ for the bottom facesheet and in the core (layer 2 to follow the notation in [16]) the axial displacement x_2 is assumed to vary linearly through the thickness. For the SYD theory, the motion is governed by

$$-EI_{tot}(1+Y)w_{,xxxx} + m(d/d_{tot})(1/g_1)w_{,xxtt} - m w_{,tt} = 0 \tag{15}$$

where $d_{tot} = h_1 + h_2 + h_3$ is the total thickness, $d = h_2 + (h_1 + h_3)/2$ is the distance between the midplanes of the facings, $I_1 = h_1^3/12$ and $I_3 = h_3^3/12$ are the moments of inertias of the top and bottom facings, and $E_1 I_1 + E_3 I_3 = EI_{tot}$. Kerwin's "geometric parameter" $Y = d^2 E_1 h_1 E_3 h_3 / EI_{tot}(E_1 h_1 + E_3 h_3)$ and the shear parameter $g_1 = (G_2/h_2)\{(1/E_1 h_1) + (1/E_3 h_3)\}$ are defined for convenience. For harmonic waves of the form $w = W \exp\{i(kx - \omega t)\}$, the dispersion relation is

$$m\omega^2 \left[1 + (d/d_{tot})(1/g_1)k^2\right] = EI_{tot}(1+Y)k^4 \tag{15}$$

For long wavelengths the dispersion curve (phase velocity versus wave number) is tangent to the line $c = k\sqrt{EI_{tot}(1+Y)/m}$. The dispersion curve tends to the asymptote $c = \sqrt{EI_{tot}(1+Y) g_1 d_{tot}/(md)}$ for short wavelengths. With the DTMM theory, the motion is governed by a 6th order equation

$$EI_{tot} w_{,xxxxxx} - EI_{tot} g_1 (1+Y) w_{,xxxx} + m w_{,xxtt} - m g_1 w_{,tt} = 0 \tag{16}$$

and the dispersion relation

$$m\omega^2 (k^2 + g_1) = EI_{tot}\left[k^6 + g_1(1+Y)k^4\right] \tag{17}$$

indicates that for long wavelengths, the dispersion curve is tangent to the line $c = k\sqrt{EI_{tot}(1+Y)/m}$ as for the SYD theory while for short wavelengths it tends to $c = k\sqrt{EI_{tot}/m}$. In other words, for long wavelengths the beam works as a single beam and for long wavelengths the two facesheets appear to be disconnected.

Backström and Nilsson [17] showed that the well-known sandwich beam theory derived by Nilsson results in a 6th order dispersion relation. The dispersion equation for that theory is bi-quadratic equation $A\omega^4 - B\omega^2 + C = 0$ with $B = I_{tot}(D_1 + D_2)k^4 + [\mu_{tot}(D_1 + D_2 + D_{tot}) + G_c h_c I_{tot}]k^2 + \mu_{tot} G_c h_c$ $A = \mu_{tot} I_{tot}$, and $C = (D_1 + D_2) D_{tot} k^6 + G_c h_c D_{tot} k^4$. In their notation, D_1 and D_2 are the bending stiffnesses per unit width of the laminates, D_{tot} is the total bending stiffness per unit with of the beam, I_{tot} is the mass moment of inertia per unit width of the beam, G_c is the shear modulus of the core, h_c is the thickness of the core, and is the total mass per unit length and width of the beam. In the following example, the facings have a thickness h_1=h_2=2 mm, an elastic modulus E_1=E_2=70 GPa and a density $\rho_1 = \rho_2$=2700 kg/m^3. The core has a thickness h_c=10 mm, a shear modulus G_c=45 MPa, and a density ρ_c=74 kg/m^3.

Fig. 4 compares the dispersion curves obtained from the Bernoulli Euler (BE), Timoshenko (T), and the Backström-Nilsson (BN) theories in three parts. Fig. 4.a shows the results for long wavelengths (k<50). The straight line is the dispersion curve for the BE theory and the other two are for the first mode of the T and BN theories. As expected the BE theory is applicable only for very long wavelengths. In this case, k<4 which corresponds to a $\lambda > 1.57$ m or more than 112 times the total thickness of the beam. For the first of the Timoshenko theory, the phase velocity c tends to the limit $\sqrt{GA/\rho A}$ =197.5 m/s while for the first mode of the BT, c appears to increase linearly with k as k increases.

From Eq. 18 we can show that, as k increases, the phase velocity tends to $c_1 = k\sqrt{(D_1 + D_2)/\mu_{tot}}$ for one mode and to $c_2 = \sqrt{D_{tot}/I_{tot}}$ for the other. Fig. 4b shows that for the first mode of the BT theory the dispersion curve is initially tangent to that for the BE theory with a bending stiffness equal to D_{tot} and then it tends to that obtained from the BE theory with a bending stiffness equal to $D_1 + D_2$. This indicates that for short wavelengths the coupling provided by the core is ineffective. Finally, Fig. 4.c shows the interactions between the two modes of the BT theory as curve veering occurs. This phenomenon occurs for wavelengths of the order of 1mm which is smaller than the thickness of the facings suggesting that the model is no longer valid at that extreme of the spectrum. The two modes of the Timoshenko beam are also shown for comparison.

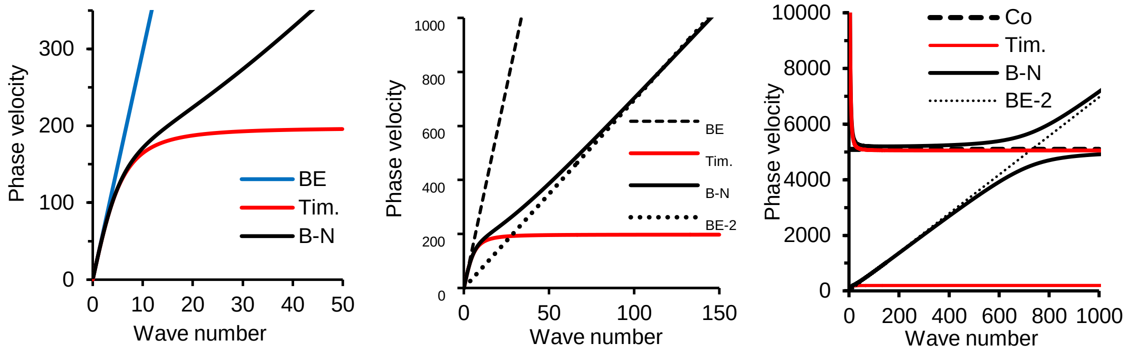

Figure 4: Dispersion relations for the BE, T, and BN beam theories (Phase velocity in m/s versus wave number in m^{-1}).

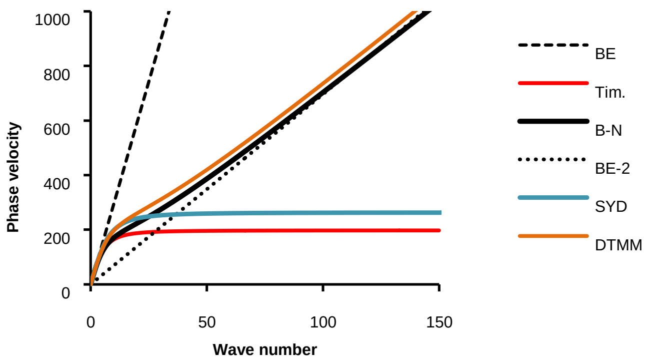

Figure 5: Comparison of five sandwich beam theories (BE, T, BN, SYD, DTMM) on the basis of harmonic wave propagation.

Fig. 5 compares the simpler SYD and DTMM theories to the theories examined previously in Fig. 4. These two theories produce the same results for long wavelengths and then diverge as k increases. The SYD behaves as the lower branch of the Timoshenko theory with a higher value of the asymptotic limit. Results for the DTMM theory are similar to those obtained using the BN theory.

3.2 Sandwich beams with transversely deformable cores

The equations of motion for two identical BE beams elastically connected in the tangential and normal directions given by Eqs. 1-6 can be written in terms of displacements. The equations simplify when written in terms of $u_a = u_1^o + u_2^o$, $u_d = u_1^o - u_2^o$, $w_a = w_1 + w_2$, $w_d = w_1 - w_2$. Two of the equations are uncoupled

$$EA\, u_{a,xx} = \rho A\, u_{a,tt}\,, \qquad EI\, w_{d,xxxx} + \rho A \ddot{w}_d + 2k_N\, w_d = 0 \tag{18}$$

and the other two are coupled

$$EA\, u_{d,xx} - k_T\left(2u_d + hw_{a,x}\right) = \rho A u_{d,tt} \qquad EI\, w_{a,xxxx} + \rho A \ddot{w}_a - hk_T\left(u_{d,x}^o + \frac{h}{2} w_{a,xx}^o\right) = 0 \tag{19}$$

Eqs. 19 govern the bending motion of the sandwich beam. The variable w_a represents the transverse displacement of the beam and u_d is a measure of the rotation of the cross section. For sandwich beams, the constants k_N and k_T can be derived in terms of the properties of the core. The simplest assumption for the deformation of the core is to assume that both the axial and transverse displacements vary linear through the thickness. This leads to the determination of k_N and k_T in terms of the material properties of the core. Then the dispersion relation is a bi-quadratic equation with terms up to k^6 like in the BN theory. For a more refined description of the deformation of the core, additional degrees of freedom are needed. Further results will be presented later.

4 LAMINATES WITH IMPERFECT INTERFACES

Laminated structures have been studied extensively since the nineteen seventies when the early papers by Pagano and Kulkarni and Pagano [18,19] first highlighted the limitations of equivalent single-layer theories, such as classical plate theory or higher-order plate theories, in modelling thick highly-anisotropic structures. Among the many models proposed in the literature, the zig-zag theories assume special relevance (e.g. [20]), since they accurately describe the complex zig-zag fields, which arise due to the multi-layered structure, using the same number of variables of equivalent single-layer theories. Early applications of the zig-zag concept to laminates with imperfect purely-elastic interfaces with $T_T \neq 0$ and $\delta_N = 0$ were presented in [7],[8]; the theories were later corrected, to make them energetically consistent, and extended to beams and plates with mixed-mode cohesive interfaces characterized by piece-wise linear tractions described by affine branches, $T_T = k_T\,\delta_T + t_T$ and $T_N = k_N\,\delta_N + t_N$, in [9],[21]. In the next sections, the model in [21] will be briefly recalled and some examples will be presented.

4.1 Multiscale modeling

The multiscale model formulated in [9][21] couples an equivalent single-layer first order shear, first order normal deformation theory and a discrete-layer cohesive-crack model, in order to efficiently describe the global behaviour of the structure and the perturbations of the local fields generated by the discontinuities of the elastic constants at the layer interfaces and the presence of imperfections. Homogenized field equations are obtained through the imposition of a-priori continuity conditions on the tractions at the layer interfaces and Hamilton principle of elastokinetics.

In [22] the model has been particularized to study the free vibrations of simply supported beams with rectangular cross section of thickness h and unit width, n layers and n-1 imperfect, purely elastic, interfaces. The interfacial traction law $T_T^i = k_T^i \delta_T^i$ relates the interfacial tractions at the *i* interface to the relative sliding displacement, δ_T^i, with k_T^i the stiffness of the *i*th interface (δ_N^i=0, for i=1..n-1).

The macro-scale displacements in the *k*th layer of the beam are:

$$u_k(x,z,t) = u^o(x,t) + z\psi(x,t) + \left[w,_x(x,t) + \psi(x,t)\right] R_{Sk}(z) \tag{20}$$
$$w_k(x,z,t) = w(x,t)$$

with:

$$R_{Sk}(z)=\sum_{i=1}^{k-1}\left[\frac{G_1(G_i-G_{i+1})}{G_iG_{i+1}}\left(z-z^i\right)+\frac{G_{i+1}}{k_T^i}\left(1+\sum_{j=1}^{i}\frac{G_1(G_j-G_{j+1})}{G_jG_{j+1}}\right)\right], \tag{21}$$

z^i the coordinate of the i[th] interface and G_i the shear modulus of the layer i. $R_{Sk}(z)$ vanishes in unidirectionally reinforced beams with fully bonded layers, when the model coincides with Timoshenko beam theory. The displacement field of Eq. (20) satisfies continuity of the shear tractions at the layer interfaces and the interfacial tractions law; the field depends on the global variables, axial and transverse displacements and bending rotation, u°,w,ψ. Using the notation applied in this paper, the dynamic equilibrium equations for the beam in the absence of surface and body loads are:

$$N,_x+I_x^0=0 \tag{20}$$

$$M,_x-V_g+I_x^1=0 \tag{21}$$

$$V_g,_x+I_z^0=0 \tag{22}$$

where N and M are the normal stress resultant and bending moment and V_g is a generalized transverse shear force, which accounts for the inhomogeneous structure and the imperfect interfaces (see [21]) and equates the classical transverse shear force, $V_g=V$, in a unidirectionally reinforced laminates with fully bonded layers; I_x^0,I_x^1,I_z^0 are inertia terms which depends on the second time derivatives of the generalized displacements, $\ddot{u}^{o},\ddot{w},\ddot{\psi}$, the mass density, material/geometrical properties and the stiffness of the interfaces; in a unidirectionally reinforced beam with no imperfections and when the reference system is centroidal, the inertia terms become $I_x^0=-\rho h\ddot{u}^{o}$, $I_x^1=-\rho I\ddot{\psi}$, $I_z^0=-\rho h\ddot{w}$ and the equilibrium equations are those of classical Timoshenko beam theory.

4.2 Dispersion curves in unidirectionally reinforced beams with elastic interfaces

The results in [22] are used here to define the dispersion equation of a unidirectionally reinforced beam with elastic constants E and G, *n* layers and *n*-1 imperfect interfaces, with $k_T^i=k_T$ for $i=1,...,n-1$. The dispersion equation is:

$$\left[\left(\frac{\omega}{k}\right)^2-\frac{E}{\rho}\right]\left\{\left(\frac{\omega}{k}\right)^4-\left[\left(\frac{\Theta_2}{k}\right)^2+\frac{E}{\rho}\Gamma\right]\left(\frac{\omega}{k}\right)^2+\frac{E}{\rho}\Gamma\left(\frac{\Theta_1}{k}\right)^2\right\}=0 \tag{25}$$

with:

$$\Theta_1^2=\frac{E}{\rho}\frac{(k^2+a)k^2}{\left[k^2+\left(\frac{1}{r^2k^2}-\frac{(n^2-1)}{n}\frac{G}{k_Th}\right)a+b\right]},\qquad \Theta_2^2=\frac{E}{\rho}\frac{(k^2+ac)k^2}{k^2+Ebh} \tag{26}$$

$$\Gamma=\left[k^2+\left(\frac{1}{r^2k^2}-\frac{(n^2-1)}{n}\frac{G}{k_Th}\right)a+b\right]\frac{1}{k^2+b}, \qquad a=\frac{1}{Er^2}\frac{G}{E}\left(\kappa+(n-1)\frac{G}{hk_T}\right)\frac{n^2}{n^2-1}\left(\frac{hk_T}{G}\right)^2,$$

$$b=\frac{1}{r^2}n^2\left(1+\frac{2}{n}\frac{K_Sh}{G}+\frac{1}{n^2-1}\left(\frac{K_Sh}{G}\right)^2\right), \quad c=1+\frac{n^2-1}{n}\frac{G}{k_Th}$$

where κ is a shear correction factor.

The first root of Eq. (25) defines the natural frequency, $\omega=c_ok$, with $c_o=\sqrt{E/\rho}$, associated to a spectrum of uniform axial vibrations of the laminate as a whole. The second and third roots, define flexural modes with frequencies:

$$\omega^{II},\omega^{III}=k\sqrt{\left(\frac{\Theta_2}{k}\right)^2+\frac{E}{\rho}\Gamma}\sqrt{\frac{1}{2}\pm\frac{1}{2}\sqrt{1-\frac{4\frac{E}{\rho}\Gamma\left(\frac{\Theta_1}{k}\right)^2}{\left[\left(\frac{\Theta_2}{k}\right)^2+\frac{E}{\rho}\Gamma\right]^2}}} \tag{27}$$

In a unidirectionally reinforced beam with no interfacial imperfections (*fully bonded limit*), $k_T\to\infty$ and $\delta_T^i\to 0$ for $i=1,...,n-1$, the dispersion equation (25) becomes that of Timoshenko beam theory, Eq. (15), and the flexural phase velocities are those depicted in Figure 3. For $k_T\to 0$ (*fully debonded limit*), a perturbation analysis of the dispersion equation (25), shows one flexural and two axial propagation modes: (a) the flexural mode of a Rayleigh beam of thickness h/n with frequency $\omega=c_0k\sqrt{rk^2/(n^2+rk^2)}$; (b) uniform axial in-phase vibrations of the *n* sub-beams with $\omega=c_ok$; (c) and a thickness shear mode [11] with zero mean value of the axial displacements over the thickness, characterized by shear deformations and interfacial sliding, with $\omega=c_ok$.

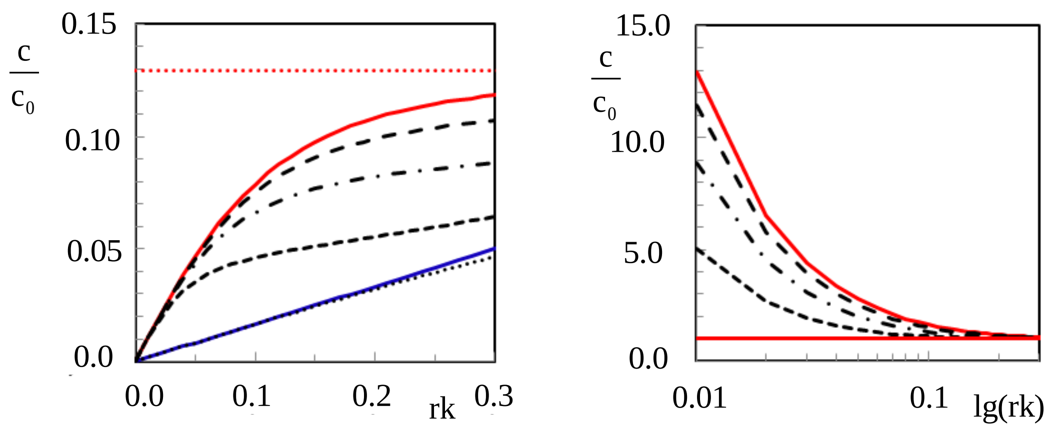

Figure 5: Non-dimensional phase velocities c/c_o versus rk, the product of the radius of gyration r and the wave number k, for a undirectionally reinforced beam with n=6 layers and 5 imperfect interfaces. (a) first flexural spectrum; (b) second flexural spectrum. The curves correspond to $k_Th/G=\infty$ (solid), 20 (dashed), 5 (dash-dot), 1 (dashed), 0 (solid). Note the different scales used for the two spectra.

Figure 5 depicts the dispersion curves for different values of the dimensionless interfacial stiffness, including the two asymptotic limits. The dispersion curves are limited from above by the solution of a fully bonded beam (Timoshenko, in red Fig. 5a,b), which coincides with the solution presented in Fig. 3. From below, the curves are limited by the fully debonded solution (Rayleigh for the first spectrum, in blue, Fig. 5a; thickness-shear mode for the second spectrum in red, Fig. 5b). The cut-off frequency of the second flexural mode, which has already been discussed in Section 2.3 for a Timoshenko beam, progressively decreases on decreasing the interfacial stiffness from the fully bonded solution, $\omega_{co}=\sqrt{\kappa Gh/\rho I}$ (Timoshenko beam), to the fully debonded solution, $\omega_{co}=0$, which would also correspond to a Timoshenko beam with vanishing shear stiffness. The reduced value of the cut-off frequency of the second flexural mode in beams with imperfect interfaces, highlights the possible relevance of the mode in dynamic problems.

Dispersion relations for beams with arbitrary lay-ups, which include the special case of sandwich beams with shear flexible cores that do not deform in the transverse direction, $w_k(x,z,t) = w(x,t)$, have been derived in [22] and results will be presented at the meeting. A more refined description of the deformations of the core, which accounts for the transverse deformability at the first-order, uses the extended model presented in [21]. Further results will be presented later.

5 CONCLUSIONS

The dynamic behaviour of multilayer structures with imperfect bonding has been examined by considering the propagation of harmonic waves. This work is applicable to laminated composite structures, sandwich structures, laminated glass, and both adhesively bonded and nailed wooden structures. Both tangential and normal relative displacements at the interfaces are considered while the existing literature usually considers tangential slip only. This study points out the challenge presented by this type of structure and the limitations of some of the existing theories. A new and improved zigzag theory is used to handle cases with many layers and imperfect interfaces.

ACKNOWLEDGEMENTS

The authors would like to acknowledge support from the Office of Naval Research Solid Mechanics Program through grants N00014-14-1-0276 and N00014-14-1-0229.

REFERENCES

[1] N.M. Newmark, C.P. Siess, I.M. Viest, Tests and analysis of composite beams with incomplete interaction, Proceedings of the Society of Experimental Stress Analysis. 9 (1951) 75–92.

[2] D. Bohnhoff, Modeling Horizontally Nail-Laminated Beams, Journal of Structural Engineering. 118 (1992) 1393–1406. doi:10.1061/(ASCE)0733-9445(1992)118:5(1393).

[3] M.Z. Aşık, S. Tezcan, A mathematical model for the behavior of laminated glass beams, Computers & Structures. 83 (2005) 1742–1753. doi:10.1016/j.compstruc.2005.02.020.

[4] L. Galuppi, G. Royer-Carfagni, Laminated beams with viscoelastic interlayer, International Journal of Solids and Structures. 49 (2012) 2637–2645. doi:10.1016/j.ijsolstr.2012.05.028.

[5] J.A. Hooper, On the bending of architectural laminated glass, International Journal of Mechanical Sciences. 15 (1973) 309–323.

[6] H.S. Norville, K.W. King, J.L. Swofford, Behavior and strength of laminated glass, Journal of Engineering Mechanics. 124 (1998) 46–53.

[7] M. Di Sciuva, Geometrically nonlinear theory of multilayered plates with interlayer slips, AIAA Journal. 35 (1997) 1753–1759.

[8] Z. Cheng, A.K. Jemah, F.W. Williams, Theory for multilayered anisotropic plates with weakened interfaces, Journal of Applied Mechanics. 63 (1996) 1019–1026.

[9] R. Massabò, F. Campi, Assessment and correction of theories for multilayered plates with imperfect interfaces, Meccanica. 50 (2015) 1045–1071. doi:10.1007/s11012-014-9994-x.

[10] A.O. Adekola, Partial interaction between elastically connected elements of a composite beam, International Journal of Solids and Structures. 4 (1968) 1125–1135.

[11] H. Erol, M. Gürgöze, Longitudinal vibrations of a double-rod system coupled by springs and dampers, Journal of Sound and Vibration. 276 (2004) 419–430.

[12] J.M. Seelig, W.H. Hoppmann, Normal mode vibrations of systems of elastically connected parallel bars, The Journal of the Acoustical Society of America. 36 (1964) 93–99.

[13] N.G. Stephen, S. Puchegger, On the valid frequency range of Timoshenko beam theory, Journal of Sound and Vibration. 297 (2006) 1082–1087.

[14] A. Bhaskar, Elastic waves in Timoshenko beams: the “lost and found”of an eigenmode, Proceedings of the Royal Society A: Mathematical, Physical and Engineering Science. 465 (2009) 239–255.

[15] J.R. Vinson, Sandwich structures: past, present, and future, in: Sandwich Structures 7: Advancing with Sandwich Structures and Materials, Springer, 2005: pp. 3–12. http://link.springer.com/chapter/10.1007/1-4020-3848-8_1 (accessed May 3, 2014).

[16] D.J. Mead, A comparison of some equations for the flexural vibration of damped sandwich beams, Journal of Sound and Vibration. 83 (1982) 363–377. doi:10.1016/S0022-460X(82)80099-0.

[17] D. Backström, A. Nilsson, Flexural Vibrations af A Three-Layer Sandwich Beam, in: O.T. Thomsen, E. Bozhevolnaya, A. Lyckegaard (Eds.), Sandwich Structures 7: Advancing with Sandwich Structures and Materials, Springer Netherlands, 2005: pp. 567–575. http://link.springer.com/chapter/10.1007/1-4020-3848-8_57 (accessed March 17, 2013).

[18] N.J. Pagano, Exact solutions for composite laminates in cylindrical bending, Journal of Composite Materials. 3 (1969) 398–411.

[19] S.V. Kulkarni, N.J. Pagano, Dynamic characteristics of composite laminates, Journal of Sound and Vibration. 23 (1972) 127–143.

[20] M. Di Sciuva, Bending, vibration and buckling of simply supported thick multilayered orthotropic plates: an evaluation of a new displacement model, Journal of Sound and Vibration. 105 (1986) 425–442.

[21] R. Massabò, F. Campi, An efficient approach for multilayered beams and wide plates with imperfect interfaces and delaminations, Composite Structures. 116 (2014) 311–324.

[22] M. Pelassa, Dynamic characteristics of anisotropic multilayered structures with interlaminar bonding imperfections via a refined generalized zig-zag model, M.S. Thesis, Polytechnic School, University of Genova, 2014.